Exact subgrid interface correction schemes for elliptic interface problems

Jae-Seok Huh and James A. Sethian*

Department of Mathematics, University of California, Berkeley, Berkeley, CA 94720

We introduce a nonconforming finite-element method for second order elliptic interface problems. Our approach applies to problems in which discontinuous coefficients and singular sources on the interface may give rise to jump discontinuities in either the solution or its normal derivative. Given a standard background mesh and an interface that passes between elements, the key idea is to construct a singular correction function that satisfies the prescribed jump conditions, providing accurate subgrid resolution of the discontinuities. Utilizing the closest point extension and an implicit interface representation by the signed distance function, an algorithm is established to construct the correction function. The result is a function that is supported only on the interface elements, represented by the regular basis functions, and bounded independently of the interface location with respect to the background mesh. In the particular case of a constant second-order coefficient, our regularization by a singular function is straightforward, and the resulting left-hand side is identical to that of a regular problem without introducing any instability. The influence of the regularization appears solely on the right-hand side, which simplifies the implementation. In the more general case of discontinuous second-order coefficients, a normalization is invoked which introduces a constraint equation on the interface. This results in a problem statement similar to that of a saddle-point problem. We employ two-level iteration as the solution strategy, which exhibits aspects similar to those of iterative preconditioning strategies.

nonconforming FEM | elliptic interface problems | interfacial singularities | level set methods

Elliptic interface problems appear in many physical applications, including Stefan problems, fluids problems, materials issues, free boundary problems, and shape optimization (1). In many moving interface problems, elliptic interface problems often arise as the interface moves, requiring repeated solutions for different interface configurations. In such problems, a moving boundary separates two different regions, such as air and ink in an ink simulation, ice and water in a crystal growth problem, or burnt and unburnt gas in a combustion problem. Boundary conditions are often supplied at and across the moving boundary and link the physics of the two different regions. These boundary conditions require delicate attention when trying to construct accurate numerical approximation schemes. Fig. 1 shows a generic example, in which an interface passes between the nodes of a nonconforming triangulated finite-element mesh.

In the above, as a model problem, we can take a Poisson equation with piecewise constant coefficient, $a_i > 0$ on each Ω_i;

$$-\nabla \cdot (a_i \nabla u) = f \quad \text{on} \quad \Omega_i \quad \text{for} \quad i = 1, 2 \qquad \text{[1]}$$

with the boundary data given on $\partial\Omega$. For well-posedness, we need additional information on the behavior of the solution on the interface. Let $\mathfrak{g}$ and $\mathfrak{h}$ be given functions defined on Γ. We assume u satisfies two jump conditions on Γ given by

$$[\![a \partial u / \partial \nu]\!] = \mathfrak{g} \quad \text{and} \qquad \text{[2a]}$$
$$[\![u]\!] = \mathfrak{h}. \qquad \text{[2b]}$$

Here, with u_i being the solution in region i, we define the jump and average operators on the interface by

$$[\![u]\!] = u_2 - u_1 \quad \text{and} \quad \{u\} = (u_2 + u_1)/2. \qquad \text{[3]}$$

If Γ is not closed, then $\Gamma \cap \partial\Omega \neq \emptyset$. We need a compatibility condition between the jump conditions and the boundary conditions. In this article, we employ the simplest form of compatibility condition, namely that $\mathfrak{g}$ and $\mathfrak{h}$ vanish on $\partial\Omega$, implying that given boundary data do not exhibit any singular behavior. As an example of our jump conditions, we note that a prescribed jump discontinuity of the flux given by Eq. **2a** frequently appears in physical phenomena involving a source (force) concentrated on the interface. Popular examples include the surface tension in a two-phase flow, the surface charge in an electrostatic problem, and latent heat absorption during dendritic solidification. A prescribed jump of the solution given by Eq. **2b** is less common in applications. One example is the flow involving volumetric change on the reaction or phase transition front.

Despite its simplicity, this problem models the general elliptic interface problem, permitting jump discontinuities in the second-order coefficient, the solution, and the flux. The key idea of our approach will remain identical with or without the lower-order terms, whose coefficient continuity affects only the higher-order regularity.

Background. How does one construct a numerical scheme to solve these problems? Because the solution may undergo a jump and lose regularity in a neighborhood containing the interface, simple interpolation cannot be done across the interface. One approach is to use an interface-conforming or body-fitted mesh. However, this may generate poor elements with bad shape factors, leading to ill-conditioned matrices and the necessity of small time steps. Worse, if the interface is moving, an elliptic solve must be performed at every time step requiring constant remeshing to the evolving front. This is not straightforward, especially in three dimensions and under topological change.

To accurately solve such problems without resorting to constant remeshing to the moving interface, a variety of sophisticated methods have been developed in recent years. These include:

- Peskin's immersed boundary method (2), its variants (3, 4)
- Immersed interface methods due to LeVeque and Li (5, 6): which are related to Mayo's method (7). The finite-element implementation of the immersed interface method can be found in Li and Ito (8).
- Extended finite-element methods (X-FEM), in which the fundamental idea is to enrich the solution space with additional basis functions, which allow discontinuities in the solution and the derivatives (9, 11).
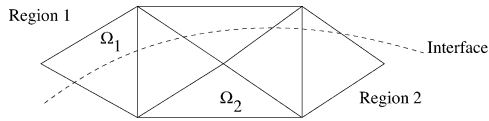
Fig. 1. Nonconforming interface passing through unstructured mesh.

These are all powerful methods to tackle this class of problems.

The Exact Subgrid Interface Correction Method [ESIC]. In this article, we present the *Exact Subgrid Interface Correction* (ESIC) scheme, which shares a similar nature with X-FEM in the sense that we construct and utilize basis functions which permit interfacial singularities. However, compared to that of an X-FEM, the construction of such basis functions presented in this paper does not require any geometric information depending on the type of the specific element employed. The interface is represented in a purely implicit manner in terms of the signed distance function, hence, the construction can be easily generalized for a wide variety of elements. However, the simplicity of the construction renders our method less robust than X-FEM, for example, our method currently does not allow crack type interfaces.

Rather than think of our method as an *enriched* FEM, unlike X-FEM, no unknown is associated with the constructed singular functions. Instead, we utilize them to recast the whole problem into a regular one with enforced singularities, which results in a better conditioned stiffness matrix. This approach of "regularization by singular correction" is also often found in spectral methods, which require sufficiently smooth solutions to achieve spectral accuracy.

To summarize, the ESIC strives to capture the virtue of existing methods while avoiding some of the drawbacks:

- First, the interface is not explicitly constructed, avoiding problems with poor shape elements and time-step stability issues.
- Second, the computed solution contains sharp discontinuities, as expected, rather than reflecting the error associated with smoothed representations of given boundary, jump, and source terms.
- Third, the method easily generalizes, and fits naturally within a level set representation of moving interfaces.

The Main Idea. To motivate our ideas, consider a constant coefficient case with $a = 1$. Suppose, for just a moment, that we are given a function with the prescribed jumps. We can then utilize the function as our correction function. That is, we can rewrite the solution of the original problem as the sum of the correction function and a solution without any singularity. Thus, instead of solving the original singular problem, we can solve the regularized problem, which is numerically sound. All the terms involving the correction function are relocated to the right-hand side, resulting an additional correction source.

The question is: How can we construct a correction function that satisfies those given jump conditions? The main idea in our work, explain in detail below, is as follows: Consider an interface element consisting of nodes $x_1, \ldots, x_n$ with the corresponding basis functions $\Upsilon_1, \ldots, \Upsilon_n$. Suppose $x_1, \ldots, x_k$ belong to Ω_1, and $x_{k+1}, \ldots, x_n$ belong to Ω_2. Let γ be a given function on the interface and $\widetilde{\gamma}$ be an extension of γ, that is, the restriction of $\widetilde{\gamma}$ on the interface is γ. With the nodal values $\widetilde{\gamma}_1, \ldots, \widetilde{\gamma}_n$ of $\widetilde{\gamma}$, we can construct a piecewise continuous function given by $-(\widetilde{\gamma}_{k+1}\Upsilon_{k+1} + \cdots + \widetilde{\gamma}_n\Upsilon_n)$ on Ω_1 and $\widetilde{\gamma}_1\Upsilon_1 + \cdots + \widetilde{\gamma}_k\Upsilon_k$ on Ω_2. Such a function is discontinuous across the interface and the amount of the jump is $\widetilde{\gamma}_1\Upsilon_1 + \cdots + \widetilde{\gamma}_n\Upsilon_n$, which is just the same as the restriction of $\widetilde{\gamma}$ on the interface, that is, γ. Thus, we can construct a function that has given jump discontinuity. In addition, if $\widetilde{\gamma}$ is the closest point extension of γ, hence, $\widetilde{\gamma}$ is constant along the interface normal, then the normal derivative of the function becomes continuous.

Now, consider the product of the above discontinuous function and the signed distance function from the interface. Because the signed distance function vanishes on the interface, the result is a continuous function. Instead, the normal derivative of the product exhibits the prescribed jump discontinuity. A linear combination of the above two functions enables us to construct a correction function with arbitrary given jump conditions.

Computational Results. Before providing a technical description of our algorithm, we first demonstrate the value of the ESIC.

Table 1 shows a comparison of our method (ESIC) with other non-conforming methods. Numerical results for X-FEM, the immersed interface method (IIM), and the immersed boundary method (IBM) are taken from Vaughan *et al.* (table 1, from ref. 12) and LeVeque and Li (table 1, from ref. 5), which corresponds to Fig. 4a of this article. We report the maximum error measured on the interface, $\|T\|_\infty$, for our method and X-FEM (with step enrichment). For IIM and IBM, we report the maximum error measured on regular nodes, $\|E\|_\infty$. Notice, in addition to regular background nodes, X-FEM uses $3.42n \sim 3.47n$ more unknowns for enriched basis function. From the results, in terms of accuracy, we can conclude that our method is comparable to X-FEM and IIM and better than IBM. The authentic advantages of our method include the simplicity in implementation, purely implicit treatment of geometry, low degree of the correction function, and better conditioned matrix.

For piecewise constant a, we normalize the problem in each subdomain. This results in an additional constraint equation, which introduces additional unknowns along the interface as in X-FEM. The resulting solution strategy is similar to a typical two-level, iterative preconditioning.

Fundamentals of ESIC: Notation and Setup. An elliptic interface problem is defined on a domain partitioned into disjoint subdomains by an interface, where the coefficients of the equation, the flux of the solution, and/or the solution itself may be discontinuous (Fig. 2). Let Ω be a bounded domain in $\mathbb{R}^d$ with Lipschitz boundary. Assume Ω is partitioned into two disjoint subdomains, Ω_1 and Ω_2. The common boundary of the subdomains is called the interface, and is denoted by Γ. We define the signed distance function ϕ from the interface by

$$\phi(x) = \begin{cases} -\inf_{y \in \Gamma}|x - y| & x \in \Omega_1 \\ \inf_{y \in \Gamma}|x - y| & \text{otherwise} \end{cases}. \qquad [4]$$

Table 1. Comparison of various methods (cf. table 1 in ref.12, for X-FEM and IBM and table 1 in ref. 5, for IIM)

	ESIC		X-FEM		IIM		IBM	
n	$\|T_n\|_\infty$	ratio	$\|T_n\|_\infty$	ratio	$\|E_n\|_\infty$	ratio	$\|E_n\|_\infty$	ratio
19	8.6325×10^{-3}		3.8397×10^{-3}		2.3908×10^{-3}		3.6140×10^{-1}	
39	2.3815×10^{-3}	3.6248	9.3787×10^{-4}	4.0943	8.3461×10^{-4}	2.8646	2.6467×10^{-2}	12.7939
79	6.1717×10^{-4}	3.8587	2.3034×10^{-4}	4.0715	2.4451×10^{-4}	3.4134	1.3204×10^{-2}	2.0045
159	1.6597×10^{-4}	3.7186	6.4061×10^{-5}	3.5965	6.6856×10^{-5}	3.6573	6.6847×10^{-3}	1.9753
319	4.1916×10^{-5}	3.9596	1.5619×10^{-5}	4.1015	1.5672×10^{-5}	4.2658	3.3393×10^{-3}	2.0018
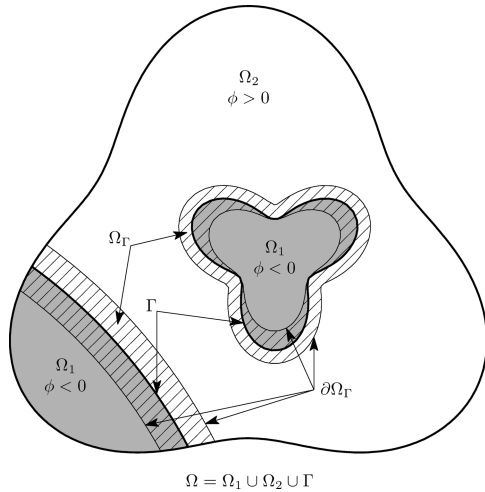
Fig. 2. A partitioned domain: subdomains, Ω_1 (gray) and Ω_2 (white), are separated by their interface, Γ. The tubular neighborhood, Ω_ϵ (shaded), is identified with the union of interface elements. In this example, the closed component of the interface contacts the boundary of Ω_ϵ.

We denote by Ω_ϵ a tubular neighborhood of Γ such that $\Gamma \subset \bar{\Omega}_\epsilon$. Assuming that any point in $\bar{\Omega}_\epsilon$ has a unique closest point on Γ, it is known that ϕ on Ω_ϵ has the same smoothness as the Γ. Our construction allows Γ to touch or even coincide with $\partial\Omega_\epsilon$.

Problems with Constant Coefficients

Regularization by Singular Correction Functions. Without loss of generality, we can assume $a = 1$ by scaling. Let $\mathcal{U} \subset H^1(\Omega)$ be the space of functions whose trace on $\partial_D\Omega$ satisfies given Dirichlet boundary data, and $\mathcal{V} \subset H^1(\Omega)$ be the space of functions with vanishing trace on $\partial_D\Omega$. We utilize $\mathcal{U}$ as the solution space for the regularized problem, and $\mathcal{V}$ acts as the space of test functions. We denote by $\mathcal{L}$ the bilinear form for the Laplacian, that is,

$$\mathcal{L}(u, v) = \int_\Omega \nabla u \cdot \nabla v \, dx,\qquad [5]$$

and by $\mathcal{L}_\epsilon$ the piecewise version of $\mathcal{L}$ defined by

$$\mathcal{L}_\epsilon(u, v) = \int_{\Omega_\epsilon \backslash \Gamma} \nabla u \cdot \nabla v \, dx.\qquad [6]$$

Note that, for $\mathcal{L}_\epsilon$, the gradient is not taken across Γ, hence, u is not required to be globally H^1. If u is H^1 on the entire domain, $\mathcal{L}_\epsilon(u, v)$ becomes identical to $\mathcal{L}(u, v)$ for any test function v. Suppose Neumann boundary data are given by a function q on $\partial_N\Omega = \partial\Omega \backslash \partial_D\Omega$. Then, the functional $\mathcal{F}$ corresponding to the regular source and the Neumann boundary condition is given by

$$\mathcal{F}(v) = \int_\Omega fv \, dx - \int_{\partial_N\Omega} qv \, dS_x.\qquad [7]$$

Let $u_\epsilon^{\mathfrak{g}}$ and $u_\epsilon^{\mathfrak{h}}$ be piecewise H^2 functions supported only on $\bar{\Omega}_\epsilon$ satisfying the jump conditions:

$$[\![u_\epsilon^{\mathfrak{g}}]\!] = 0, \quad [\![\partial u_\epsilon^{\mathfrak{g}}/\partial\nu]\!] = \mathfrak{g},\qquad [8a]$$

$$[\![u_\epsilon^{\mathfrak{h}}]\!] = \mathfrak{h}, \quad [\![\partial u_\epsilon^{\mathfrak{h}}/\partial\nu]\!] = 0.\qquad [8b]$$

Define an additional source term originating from the correction function $u_\epsilon = u_\epsilon^{\mathfrak{g}} + u_\epsilon^{\mathfrak{h}}$ by

$$\mathcal{F}_\epsilon(v) = -\mathcal{L}_\epsilon(u_\epsilon, v) - \int_\Gamma \mathfrak{g}v \, dS_x$$
$$= -\mathcal{L}_\epsilon(u_\epsilon^{\mathfrak{h}}, v) - \mathcal{L}_\epsilon(u_\epsilon^{\mathfrak{g}}, v) - \int_\Gamma \mathfrak{g}v \, dS_x.\qquad [9]$$

Notice, we assume $u_\epsilon^{\mathfrak{g}}$ and $u_\epsilon^{\mathfrak{h}}$ are continuous on each subdomain, but their normal derivatives can be discontinuous across $\partial\Omega_\epsilon$. Let $q_\epsilon^{\mathfrak{g}} = \partial u_\epsilon^{\mathfrak{g}}/\partial n|_{\partial\Omega_\epsilon}$. By taking the integration by parts for $\mathcal{L}_\epsilon(u_\epsilon^{\mathfrak{g}}, v)$, we derive an alternative representation for $\mathcal{F}_\epsilon$,

$$\mathcal{F}_\epsilon(v) = -\mathcal{L}_\epsilon(u_\epsilon^{\mathfrak{h}}, v) + \int_{\Omega_\epsilon \backslash \Gamma} \Delta u_\epsilon^{\mathfrak{g}} v \, dx + \int_{\partial\Omega_\epsilon} q_\epsilon^{\mathfrak{g}} v \, dS_x.\qquad [10]$$

Here, we take the Laplacian of $u_\epsilon^{\mathfrak{g}}$ in the piecewise manner. The second representation does not involve any explicit integral over Γ. Instead, our functional $\mathcal{F}_\epsilon$ contains the distribution source $q_\epsilon^{\mathfrak{g}}$ on the boundary of Ω_ϵ. The integration by parts for $\mathcal{L}_\epsilon(u_\epsilon^{\mathfrak{h}}, v)$ does not produce any distribution on Γ; its flux difference vanishes. Thus, such $\mathcal{F}_\epsilon$ corresponds an L_2 source supported only on Ω_ϵ accompanied by an H^{-1} distribution supported on $\partial\Omega_\epsilon$, associated to a flux jump.

Let us find a *regular*[†] solution $u_R \in \mathcal{U}$ satisfying, for all $v \in \mathcal{V}$,

$$\mathcal{L}(u_R v) = \mathcal{F}(v) + \mathcal{F}_\epsilon(v).\qquad [11]$$

The problem is well-posed, and the solution u_R is continuous on the entire domain and piecewise H^2 in each of $\bar{\Omega}_\epsilon$, $\Omega_1 \backslash \Omega_\epsilon$, and $\Omega_2 \backslash \Omega_\epsilon$. This is due to the L_2 regularity of the right-hand side of Eq. 11 in each of those subdomains. We can observe that $u = u_R + u_\epsilon$ satisfies $-\Delta u = f$ on each Ω_i. The jump conditions on Γ, $[\![\partial u/\partial\nu]\!] = \mathfrak{g}$ and $[\![u]\!] = \mathfrak{h}$, are enforced by the singular correction function, u_ϵ. In our construction, the role of the singular correction function is to replace the distributions on Γ, given in terms of $\mathfrak{g}$ and $\mathfrak{h}$, with an L_2 function supported on Ω_ϵ (on interface elements) and a distribution supported on $\partial\Omega_\epsilon$ (on the boundary of those interface elements); hence, the resulting problem is conforming to the given background mesh.

Note that $\mathcal{L}$ and $\mathcal{F}$ do not involve any information related to the location of Γ; they remain identical to those from regular conforming problems. The only interface-dependant term is the correction source, $\mathcal{F}_\epsilon$. Because our u_ϵ is supported only on the interface elements, the computational cost for the evaluation of Eq. **10** is negligible in the entire procedure. In general, the integrand in Eq. **10** is discontinuous across Γ, but this adds only minor difficulty in our method.

Construction of Singular Correction Functions. The remaining question is to construct well behaved singular correction functions; that is, for any given interface jumps on an arbitrary interface Γ within any given support Ω_ϵ, we should construct the correction functions $u_\epsilon^{\mathfrak{g}}$ and $u_\epsilon^{\mathfrak{h}}$ whose H^2 norms are well bounded independently of the location of Γ within Ω_ϵ (Fig. 3).

Given a background mesh, we denote by Υ_i the basis function associated to a node x_i satisfying

$$\Upsilon_i(x_j) = \delta_{ij} \quad \text{and} \quad \sum_i \Upsilon_i(x) = 1.\qquad [12]$$

The second condition simply means the basis functions can resolve a constant function exactly. These requirements are satisfied by almost every basis function used in practice including all isoparametric elements of any order. We use $\{\Upsilon_i\}$ only for the representation of the extension of the given interface jumps and for the construction of the singular correction functions; the regular solution u_R, the regular source f, and the signed distance function ϕ can be represented by different basis functions.

We begin with the implicit representation of interfacial functions by the *closest point extension* (Fig. 3). Let γ be a function

---

[†] Even though we call it a regular solution, u_R is not globally regular; it has the jump in the normal derivative across $\partial\Omega_\epsilon$ given by $-\partial u_\epsilon/\partial n|_{\partial\Omega_\epsilon}$. But, the equation is as good as a globally regular one, because Ω_ϵ can be chosen to conform to any given background mesh; that is, for any given fixed background mesh, we choose Ω_ϵ to be the set of all elements that contains Γ, then the mesh is conforming to $\partial\Omega_\epsilon$. Hence, the distribution on $\partial\Omega_\epsilon$ can be well treated on a conforming mesh.
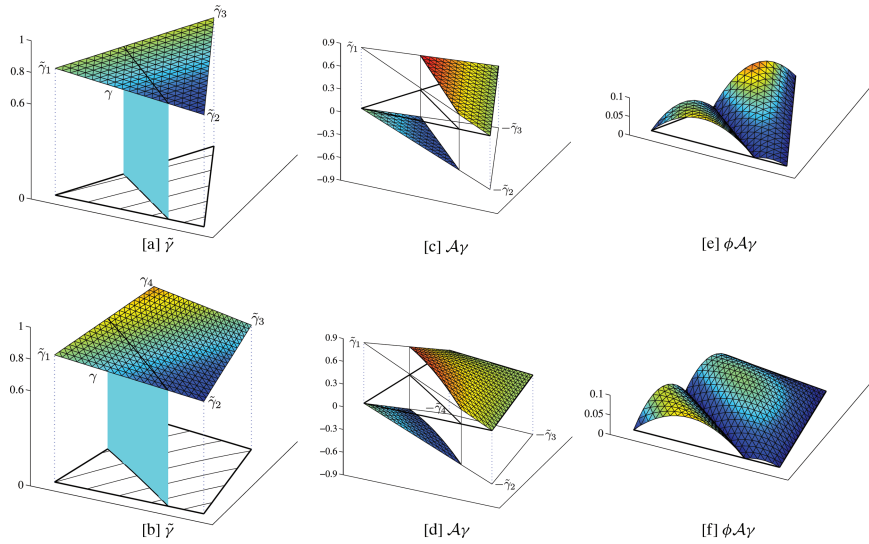
Fig. 3. The construction of correction functions based on piecewise linear basis functions. (*a*) Extension of given function γ on the interface in a triangular element. (*c*) Piecewise linear function with the prescribed jump. (*e*) Piecewise quadratic function with the prescribed jump in the normal derivative. (*b*, *d*, and *f*) Same operations for a quadrilateral element.

defined on Γ, its closest point extension $\widetilde{\gamma}$ on Ω_ϵ is defined by $\widetilde{\gamma}(x) = \gamma(x^*)$, where $x^* = x - \phi(x)\nabla\phi(x)$ is the closest point of x on Γ. This extension renders $\widetilde{\gamma}$ constant along the normal directions of Γ, that is, $\nabla\widetilde{\gamma}\cdot\nabla\phi = 0$ in Ω_ϵ. We represent the discretization of $\widetilde{\gamma}$ by

$$\widetilde{\gamma} = \sum_i \widetilde{\gamma}_i \Upsilon_i, \qquad [13]$$

Fig. 4. Solutions of an example problem with constant $a = 1$ for various interfaces: The exact solution is given by $u_1 = 1$ and $u_2 = 1 - \log(2r)$. The triangular background mesh is generated from a 40×40 uniform grid. Solutions exhibit sharp subgrid resolutions of the interfacial singularities.

where $\widetilde{\gamma}_i$ is $\gamma(x_i^*)$. Thus, the first stage of the numerical extension is to find the closest point x_i^* of a node x_i on the interface elements. Then, the value $\widetilde{\gamma}_i$ can be obtained by the interpolation associated with the background mesh. Obviously, the $\|\widetilde{\gamma}\|_{\Omega_\epsilon\infty}$ is bounded by $\|\gamma\|_{\Gamma,\infty}$.

Functions with Prescribed Jumps and Continuous Fluxes. In this section, we present a linear mapping $\mathcal{A}$ which, from a given function γ on Γ, constructs a function with the prescribed jump and continuous normal derivative. Let Ψ_1 be a continuous function on Ω such that $\Psi_1 = 1$ on $\Omega_1\backslash\Omega_\epsilon$ and $\Psi_1 = 0$ on $\Omega_2\backslash\Omega_\epsilon$. Assume Ψ_1 is sufficiently regular in Ω_ϵ. Define Ψ_2 by $\Psi_1 + \Psi_2 = 1$. Consider a linear mapping $\mathcal{A}$ given by

$$(\mathcal{A}\gamma)(x) = \begin{cases} -\widetilde{\gamma}(x)\Psi_2(x) & x \in \Omega_1 \\ \widetilde{\gamma}(x)\Psi_1(x) & x \in \Omega_2 \end{cases}. \qquad [14]$$

Then, $\mathcal{A}\gamma$ is continuous on each Ω_i, vanishes on $\Omega\backslash\Omega_\epsilon$, and satisfies the jump conditions;

$$[\![\mathcal{A}\gamma]\!] = \widetilde{\gamma}(\Psi_1 + \Psi_2)|_\Gamma = \widetilde{\gamma}|_\Gamma = \gamma. \qquad [15]$$

Since $\nabla(\Psi_1 + \Psi_2)\cdot\nabla\phi = 0$ and $\nabla\widetilde{\gamma}\cdot\nabla\phi = 0$ on Ω_ϵ,

$$[\![\partial\mathcal{A}\gamma/\partial\nu]\!] = 0. \qquad [16]$$

Before we present the numerical implementation of $\mathcal{A}$ in terms of $\{\Upsilon_i\}$, observe that the above aspects are satisfied by the following construction of Ψ_1 and Ψ_2:

$$\Psi_1 = \sum_{\phi_i<0} \Upsilon_i \quad \text{and} \quad \Psi_2 = \sum_{\phi_i\geq0} \Upsilon_i, \qquad [17]$$

where ϕ_i is the signed distance at x_i. A naive implementation of $\mathcal{A}$ is just to multiply them by $\sum \widetilde{\gamma}_i \Upsilon_i$. But, this results in an increase in the degree of the polynomial. We present the following implementation for $\mathcal{A}$ which maintains the same degree as $\{\Upsilon_i\}$:

$$(\mathcal{A}\gamma)(x) = \begin{cases} -\sum_{\phi_i\geq0} \widetilde{\gamma}_i \Upsilon_i(x) & x \in \Omega_1 \\ \sum_{\phi_i<0} \widetilde{\gamma}_i \Upsilon_i(x) & x \in \Omega_2 \end{cases}. \qquad [18]$$

Notice that, if an interface happens to be conforming to the background mesh, this algorithm produces an result identical to the imposition of Dirichlet boundary conditions in standard finite

element methods. Thus, we consider a solution jump condition as a *generalized Dirichlet condition*, which can be imposed on the interface.

Continuous Functions with Prescribed Flux Jumps. With the mapping $\mathcal{A}$ obtained in the previous section, we consider the linear operator $\phi\mathcal{A}$, operator $\mathcal{A}$ weighted by the signed distance function. Since ϕ vanishes on the interface, so does $\phi\mathcal{A}\gamma$. Hence, the result is a function continuous on the entire domain, supported only on Ω_ϵ. Since $\nabla\phi\cdot\nabla\phi = 1$, $\nabla(\phi\mathcal{A}\gamma)\cdot\nabla\phi = \mathcal{A}\gamma + \phi\nabla\mathcal{A}\gamma\cdot\nabla\phi$. Hence,

$$[\![\,\partial(\phi\mathcal{A}\gamma)/\partial\nu\,]\!] = [\![\,\mathcal{A}\gamma\,]\!] = \gamma. \qquad [19]$$

The linear operators $\mathcal{A}$ and $\phi\mathcal{A}$ can be applied to the solution jump condition and the flux jump condition respectively and independently. Thus, the correction functions $u_\epsilon^{\mathfrak{g}}$ and $u_\epsilon^{\mathfrak{h}}$ are given by

$$u_\epsilon^{\mathfrak{g}} = \phi\mathcal{A}\mathfrak{g} \quad \text{and} \quad u_\epsilon^{\mathfrak{h}} = \mathcal{A}\mathfrak{h}. \qquad [20]$$

Recall that $\{\Upsilon_i\}$ depends only on the choice of Ω_ϵ, independently of the location of Γ with respect to Ω_ϵ. An extended function shows well bounded behaviors depending only on the original function on Γ and the geometric quantities of Γ, for example, curvatures. The construction works fine even in the extreme case that Γ is a part of $\partial\Omega_\epsilon$. In the finite-element implementation, the evaluation of the constructed function is interface-implicit; that is, except for the extension, those procedures do not involve any explicit computation regarding the location of Γ. All quantities are represented by nodal values and the basis functions of the background mesh, which implies that the idea of our construction can be applied to a variety meshes in arbitrary dimensions. Thus, our construction of u_ϵ is numerically stable, efficient, and simple in the implementation.

Implementation: Linear Bases with Quadratic Refinements. Numerical experiments were performed with piecewise linear bases (for every representation including signed distance functions) on a triangular mesh. On each interface element, the constructed $u_\epsilon^{\mathfrak{h}}$ from piecewise linear $\{\Upsilon_i\}$ is a linear polynomial in each subdomain, and the resulting $u_\epsilon^{\mathfrak{g}}$ becomes a quadratic polynomial in each subdomain.

Suppose the exact solution is a piecewise linear function. Then, with $\mathfrak{g} \neq 0$, the regularized solution u_R is a quadratic polynomial on each interface element. To capture the exact solution in such a case, we added quadratic basis functions for the solution space so that the discrete solution space can represent a quadratic polynomial on each interface element. For triangular mesh, this can be accomplished by adding quadratic *hierarchical* basis functions on the edges containing the interface. We can observe that a similar local refinement is employed in X-FEM (10). The resulting stiffness matrix consists of: (*i*) the stiffness matrix of the linear background basis, which is always identical independently of the location of the interface, and (*ii*) the small auxiliary part which corresponds to the enriched quadratic basis functions. The refinement does not produce any harmful effect: the matrix remains symmetric positive definite and well conditioned.

The resulting linear equation can be solved by various methods: we chose a conjugate gradient method. Preconditioning and fast solution methods can be applied also as regular problems. Results show sharp subgrid resolution of interfacial singularities. The measured convergence is a fraction between 1 and 2, and approaches to the expected second order as variations in the geometry and in the interfacial data decrease. We suspect one major reason of the degradation in the convergence rate is our choice of a piecewise linear representation for signed distance functions, where normal vectors are discontinuous and typically exhibit oscillations. Local errors near the interfaces maintain the same order of magnitude as the far-field data. This is one preferred
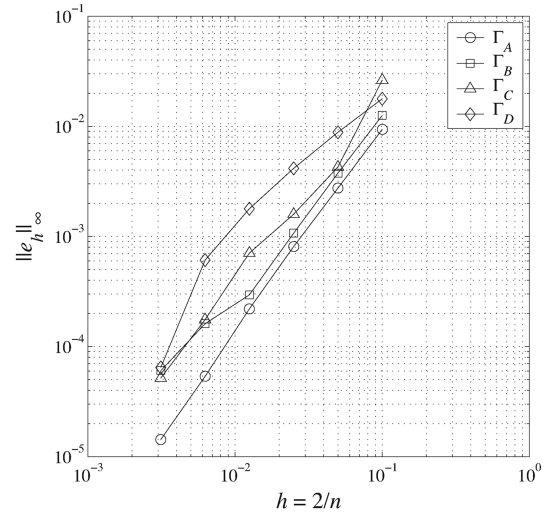
(a) Test of convergence
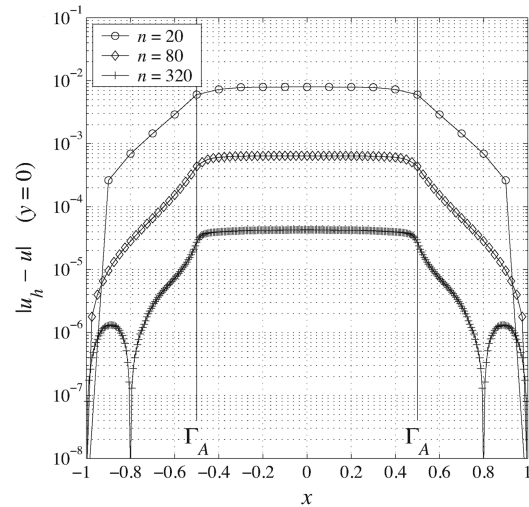
(b) Pointwise L_∞ error on $y = 0$ for $\Gamma_{\mathcal{A}}$

Fig. 5. Results for constant $a = 1$ (same problem as Fig. 4). (*a*) Γ_A (circle) exhibits the most straight convergence with the rate, 1.88. (*b*) The method does not produce any peak of large local error near the interface.

characteristic of our method compared with regularization methods that typically involve a significant loss of accuracy near the interface and can lose multiple correct digits locally.

Problems with Piecewise Constant a

Normalization. Utilizing the solution scheme derived for problems with $a = 1$, we present a solution strategy for a more general class of problems given by Eq. **1** with piecewise constant a. First, we introduce a scaled unknown $\bar{u}$ defined by

$$\bar{u} = \frac{a_i}{\{a\}}u \quad \text{on} \quad \Omega_i \quad \text{for} \quad i = 1, 2. \qquad [21]$$

Then, we obtain the normalized problem given by

$$-\Delta\bar{u} = f/\{a\} \quad \text{on} \quad \Omega_i \quad \text{for} \quad i = 1, 2, \qquad [22a]$$

$$[\![\,\partial\bar{u}/\partial\nu\,]\!] = \mathfrak{g}/\{a\}, \quad \text{and} \qquad [22b]$$

$$[\![\,\bar{u}/a\,]\!] = \mathfrak{h}/\{a\}. \qquad [22c]$$

We can decouple $\bar{u}$ and a in **Eq. 22c** by utilizing

$$[\![\,\bar{u}/a\,]\!] = [\![\,\bar{u}\,]\!]\{1/a\} + [\![\,1/a\,]\!]\{\bar{u}\} = \frac{\{a\}}{a_1 a_2}\left([\![\,\bar{u}\,]\!] - \frac{[\![\,a\,]\!]}{\{a\}}\{\bar{u}\}\right),$$
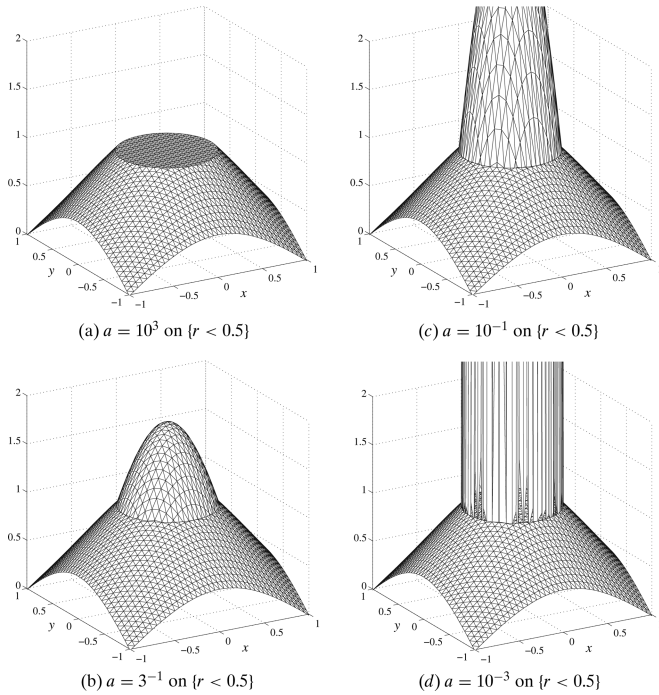
Fig. 6. Solutions of problems with discontinuous a. $a = 1$ on $\{r > 0.5\}$. The exact solution is given by $1 - \log(3/4 + r^2)$ for $r > 0.5$ and $1 - \log(3/4 + r^2)/a$ for $r < 0.5$. GMRES for the outer iteration converged within $10 \sim 15$ iterations depending on a, independently of the mesh size. In (d), because of the large scaling factor of $O(10^3)$, the L_∞ error on $\{r < 0.5\}$ appears to be large. However, its convergence is clear, and the error in the a-weighted (energy) norm is small.

which results in

$$[\![\bar{u}]\!] = \mathfrak{h}\frac{a_1 a_2}{\{a\}^2} + \alpha\{\bar{u}\} \quad \text{where} \quad \alpha = \frac{[\![a]\!]}{\{a\}}. \qquad \textbf{[23]}$$

The dimensionless constant α is always in $(-2, 2)$ for any positive a_1 and a_2. Notice, the right-hand side of Eq. **23** contains the average trace of the unknown itself. To resolve the difficulty, we introduce a constraint γ defined on Γ satisfying $\gamma = \{\bar{u}\}$. Then, $\bar{u}$ satisfies

$$-\Delta\bar{u} = \bar{f} \quad \text{on} \quad \Omega_i \quad \text{for} \quad i = 1, 2, \qquad \textbf{[24a]}$$

$$[\![\partial\bar{u}/\partial\nu]\!] = \bar{\mathfrak{g}}, \qquad \textbf{[24b]}$$

$$[\![\bar{u}]\!] = \bar{\mathfrak{h}} + \alpha\gamma, \qquad \textbf{[24c]}$$

where $\bar{f} = f/\{a\}$, $\bar{\mathfrak{g}} = \mathfrak{g}/\{a\}$, and $\bar{\mathfrak{h}} = \mathfrak{h}a_1 a_2/\{a\}^2$. Notice, given boundary conditions should be scaled appropriately; for Dirichlet conditions, the scaling factor is $a_i/\{a\}$ on each Ω_i. The scaling factor for Neumann conditions is $1/\{a\}$ on the entire domain (Fig. 5), and results are given in Fig. 6.

Particular and Homogeneous Problems. It is more comprehensive to rewrite the normalized solution $\bar{u}$ as the sum of the *particular solution* $\bar{u}^0$ and the *homogeneous solution* $\bar{u}^\gamma$ such that $\bar{u}^0$ carries all the given data: $\bar{f}, \bar{\mathfrak{g}}, \bar{\mathfrak{h}}$, and given boundary conditions. That is, $\bar{u}^0$ is the solution of the particular problem:

$$-\Delta\bar{u}^0 = \bar{f} \quad \text{on} \quad \Omega_i \quad \text{for} \quad i = 1, 2, \qquad \textbf{[25a]}$$

$$[\![\partial\bar{u}^0/\partial\nu]\!] = \bar{\mathfrak{g}}, \quad [\![\bar{u}^0]\!] = \bar{\mathfrak{h}} \qquad \textbf{[25b]}$$

and *given nonhomogeneous* boundary conditions. Let $\gamma^0 = \{\bar{u}^0\}$, then $\{\bar{u}\} = \gamma^0 + \{\bar{u}^\gamma\}$. Then, the homogeneous solution $\bar{u}^\gamma$ satisfies *homogeneous* boundary conditions and

$$-\Delta\bar{u}^\gamma = 0 \quad \text{on} \quad \Omega_i \quad \text{for} \quad i = 1, 2, \qquad \textbf{[26a]}$$

$$[\![\partial\bar{u}^\gamma/\partial\nu]\!] = 0, \quad [\![\bar{u}^\gamma]\!] = \alpha\gamma, \qquad \textbf{[26b]}$$

and the constraint γ satisfies $\{\bar{u}^\gamma\} - \gamma = -\gamma^0$. If $\alpha = 0$, then $\bar{u}^\gamma = 0$ is the unique solution of the homogeneous problem, i.e. $\bar{u} = \bar{u}^0$.

Structure of Homogeneous Problems. Because homogeneous problems do not involve any flux jump, the additional source term $\mathcal{F}_\epsilon$ has a simpler form,

$$\mathcal{F}_\epsilon(v) = -\alpha\mathcal{L}_\epsilon(\mathcal{A}\gamma, v). \qquad \textbf{[27]}$$

Because of the trivial regular source and the homogeneous Neumann condition, $\mathcal{F}(v) = 0$. Denote by $\mathcal{M}$ the linear average trace operator, which is identical to the usual trace on Γ for regular functions. We identify $\mathcal{L}$ and $\mathcal{L}_\epsilon$ with the corresponding linear operators. Notice, $\mathcal{L}$ includes the homogeneous Dirichlet boundary condition. Then, the (discretized) homogeneous problem is regularized to

$$\begin{pmatrix} \mathcal{L} & \alpha\mathcal{L}_\epsilon\mathcal{A} \\ \mathcal{M} & \alpha\mathcal{M}\mathcal{A} - I \end{pmatrix} \begin{pmatrix} \bar{u}_R^\gamma \\ \gamma \end{pmatrix} = \begin{pmatrix} 0 \\ -\gamma^0 \end{pmatrix}. \qquad \textbf{[28]}$$

Here, we utilize the fact that $\{\bar{u}^\gamma\} = \{\bar{u}_R^\gamma\} + \alpha\{\mathcal{A}\gamma\}$.

Although the stiffness matrix is, in general, not symmetric, we can use a two-level iteration strategy on the symmetric matrix $\mathcal{L}\bar{u}_R^\gamma = -\alpha\mathcal{L}_\epsilon\mathcal{A}\gamma$, together with a linked associated smaller nonsymmetric constraint equation $(I - \alpha\mathcal{M}\mathcal{A} + \alpha\mathcal{M}\mathcal{L}^{-1}\mathcal{L}_\epsilon\mathcal{A})\gamma = \gamma^0$; judicious use of GMRES and preconditioning strategies provides an efficient algorithm.

We have presented a method for solving elliptic interface problems on nonconforming unstructured meshes. Our method is robust, accurate, and does not require an explicit representation of the subgrid interface geometry. In addition, our method shows strong stability for both huge and tiny coefficient ratios, and hence enables application to the solution of boundary value problems on extended domains, in which we view the virtual boundary as an interface with given Dirichlet or Neumann conditions imposed as jump conditions.

1. Sethian JA (1999) *Level Set Methods and Fast Marching Methods* (Cambridge Univ Press, New York).
2. Peskin CS (1977) Flow patterns around heart valves: A numerical method. *J Comput Phys* 25:220–252.
3. Lai M-C, Peskin CS (2000) An immersed boundary method with formal second-order accuracy and reduced numerical viscosity. *J Comput Phys* 160:705–719.
4. Tornberg A-K, Shelley MJ (2004) Simulating the dynamics and interactions of flexible fibers in stokes flows. *J Comput Phys* 196:8–40.
5. LeVeque RJ, Li Z (1994) The immersed interface method for elliptic equations with discontinuous coefficients and singular sources. *SIAM J Numer Anal* 31:1019–1044.
6. LeVeque RJ, Li Z (1997) Immersed interface methods for Stokes flow with elastic boundaries or surface tension. *SIAM J Sci Comput* 18:709–735.
7. Mayo A (1984) The fast solution of poisson's and the biharmonic equations on irregular regions. *SIAM J Numer Anal* 21:285–299.
8. Li Z, Ito K (2006) *The Immersed Interface Method: Numerical Solutions of PDEs Involving Interfaces and Irregular Domains* (Frontiers in Applied Mathematics) (Soc Indust Appl Math, Philadelphia).
9. Belytschko T, Moës N, Usui S, Parimi C (2001) Arbitrary discontinuity in finite elements. *Int J Numer Meth Eng* 50:993–1013.
10. Chessa J, Wang H, Belytschko T (2003) <53><53><53>. *Int J Num Meth Eng* 57:1015–1038.
11. Moës N, Dolbow J, Belytschko T (1999) A finite element method for crack growth without remeshing. *Int J Num Meth Eng* 46:131–150.
12. Vaughan BL, Jr, Smith BG, Chopp DL (2006) A comparison of the extended finite element method with the immersed interface method for elliptic equations with discontinuous coefficients and singular sources. *Comm Appl Math Comp Sci* 1:207–228.